# Treatment of Oil Palm Empty Fruit Bunch Regenerated Cellulose Biocomposite Films using Methacrylic Acid

Nur Liyana Izyan Zailuddin,[a] Salmah Husseinsyah,[a,*] Farah Norain Hahary,[a] and Hanafi Ismail [b]

Regenerated cellulose (RC) biocomposite films from oil palm empty fruit bunch (OPEFB) and microcrystalline cellulose (MCC) were prepared using ionic liquid. N,N-Dimethylacetamide (DMAc) and Lithium Chloride (LiCl) were used to dissolve the regenerated cellulose at room temperature. The effects of OPEFB content and chemical modification using methacrylic acid (MAA) on the X-ray diffraction, tensile properties, morphology, thermal properties, and Fourier transform infrared spectroscopy (FTIR) results for RC biocomposite films were investigated. The chemical modification of OPEFB using MAA enhanced the properties of the treated RC biocomposite films. At 2 wt.% of OPEFB both of the RC biocomposite films showed the highest crystallinity index, tensile strength, modulus of elasticity, and thermal stability. The treated RC biocomposite films had a higher crystallinity index, tensile strength, modulus of elasticity, and thermal properties than the untreated RC biocomposite films. The $T_{dmax}$ of treated RC biocomposite films with MAA was higher than that of untreated RC biocomposite films. This indicates that treated biocomposite films had higher thermal stability. The enhancement of interfacial interaction and the dispersion of treated RC biocomposite films with MAA were revealed by scanning electron microscopy (SEM). The FTIR spectra of treated RC biocomposite films indicated interaction between cellulose from OPEFB and MCC with MAA.

*Keywords: Oil palm empty fruit bunch; Regenerated cellulose; Methacrylic acid; Biocomposite films*

*Contact information: a: School of Materials Engineering, Universiti Malaysia Perlis, 02600 Jejawi, Arau, Perlis, Malaysia; b: School Material and Mineral Resources Engineering, UniversitiSains Malaysia, Nibong Tebal, 14300, Penang; *Corresponding author: irsalmah@unimap.edu.my*

## INTRODUCTION

The research and development of biodegradable polymer materials has drawn considerable attention because of a new sustainable development concept (Zhang *et al.* 2012; Soheilmoghaddam *et al.* 2014a,b). More of these biopolymers are being studied to investigate their potential for use as alternative materials to the diminishing petroleum and fossil fuels.

Cellulose is a naturally occurring resource polymer with the chemical formula $C_6H_{10}O_5$, and has gained interest for use mainly as a natural fiber reinforcement (Nishiyama *et al.* 2002). Its properties of biorenewability and biodegradability can lead to a mass production that is environmentally friendly, without the emission of harsh pollutants to the surroundings (Kalia *et al.* 2011). In recent years, a new type of composite known as an all-cellulose composite has begun to attract attention. The reinforcement and matrix phases are both in the same polymer forms (*e.g.*, cellulose). The products are called self-reinforced polymeric matrix materials (SRPMs) (Kmelty *et al.* 2010). SPRMs have better

performance and cost balance compared with traditional composites. In this approach, part of the polymer fiber is melted and then recrystallized into a matrix, which bonds the fibers together and forms a perfect interface (Ward and Hine 2004). Nishino *et al.* (2004) were the first to develop this approach for cellulosic materials. In their study, they reported that dissolved kraft fibers used the cellulose solution as a binder matrix for uniaxially aligned ramie fibers (Nishino *et al.* 2004). All-cellulose composites could also be produced by the partial dissolution of cellulose, whereby the surface layer of cellulose fiber is partially dissolved and regenerated to form the matrix portion (Huber *et al.* 2012). Dulchemin *et al.* (2009) reported the partially dissolved micro-crystallinity cellulose in DMAc/LiCl and precipitated the dissolved portion to form a matrix around the non-dissolved portion. This concept has led to the production of regenerated cellulose biocomposite films.

Regenerated cellulose is known as man-made cellulose, and was introduced in 1846 when Karl-Friedrich Schönbein discovered cellulose nitrate (Röder *et al.* 2009). The steps of cellulose regeneration began when some parts of the cellulose began to swell when dissolving into a particular solvent. This swollen cellulose was transformed into the matrix phase, covering the non-dissolved part of cellulose that acts as reinforcement. After the partial dissolution of cellulose, the solvent was removed using a coagulant (for example, water) followed by evaporative drying. This cellulose regeneration is crucial, as it controls the precipitant of the final cellulose phase dissolution (Huber *et al.* 2012).

To produce regenerated cellulose, the cellulose must dissolve into suitable solvents. Some recently used solvents include N-methylmorpholine-N-oxide (NMMO) (Biganska and Navard 2002; Zhao *et al.* 2007) and N-dimethylacetamide/lithium chloride (DMAc/LiCl) (Zhang *et al.* 2012). A study by Liu *et al.* (2015) showed that regenerated cellulose that was prepared from the ionic liquid 1-butyl-3-methylimidazolium acetate([Bmim]Ac) solution using anti-solvent compressed $CO_2$ results in a more homogeneous texture of regenerated cellulose. Many reports have been conducted regarding the use of DMAc/LiCl as a cellulose dissolution system. For instance, Zhao *et al.* (2014) studied the reinforcement of all-cellulose nanocomposite films with DMAc/LiCl-dissolved regenerated cellulose as the matrix. Their study showed that the tensile strength of the nano-films increased by varying the cellulose nanocomposite films (Zhao *et al.* 2014). Another study reported by Ghaderi *et al.* (2014) on all-cellulose nanocomposite films made from bagasse cellulose showed that water vapor permeability increased, making it a possible material for use as an application for cellulose-based food packaging.

The palm oil industry business is considered to be one of the largest agriculture businesses in Malaysia. Recently in 2012, the total amount of palm oil production reached up to 18.8 million tons, which led to biomass lignocellulose waste of about 43.24 million tons (Sulaiman *et al.* 2011; Chang 2014). These residues are in the form of abundantly available oil palm empty fruit bunch (OPEFB), oil palm fiber, and other lignocellulosic wastes (Ariffin *et al.* 2008; Sahari and Sapuan 2011). OPEFB is a lignocellulosic material composed of cellulose, hemicelluloses, and lignin, with cellulose dominant in the composition (Geng 2013). The high content of cellulose makes OPEFB easily bio-converted into valuable products.

Generally, cellulose cannot be dispersed uniformly, especially in non-polar polymer media or most solvents, because of its hydrophilic nature. For film productions, it is important for cellulose to be compatible with and dissolve into particular solvents. This can be achieved by modifying the hydroxyl part of cellulose, whereby the available hydroxyl groups can be employed for modification as they can act as chemical handles.

These hydroxyl groups can be tuned by different pretreatment methods. For example, the reaction acetic anhydride (acetylation) substitutes the hydroxyl group of cellulose with the acetyl group to make cellulose hydrophobic (Li *et al.* 2007).

In this study, methacrylic acid (MAA) was used to alter the hydroxyl groups in cellulose to allow for better solvent dissolubility in producing biocomposite films. The aim of this research was to study the effect of different OPEFB contents of regenerated cellulose biocomposite films using N, N-dimethylacetamide/lithium chloride (DMAc/ LiCl) based on X-ray diffraction, tensile properties, morphology, thermal properties, and Fourier transform infrared spectroscopy analysis.

## EXPERIMENTAL

### Materials

Oil palm empty fruit bunch (OPEFB) was obtained from the Malaysian Palm Oil Board (MPOB), Bangi, Selangor. After being ground with a ball mill, the average particle size of OPEFB was 35 μm, measured using a Malvern Size analyzer, UK. Microcrystalline cellulose (MCC) was supplied by Aldrich, USA. Sodium hydroxide (NaOH), ethanol ($C_2H_5OH$), and sulfuric acid ($H_2SO_4$) were obtained from HmbG® Chemicals, Germany. Sodium chlorite ($NaClO_2$) and methacrylic Acid (MAA) were supplied by Sigma-Aldrich, USA. Acetic acid was obtained from BASF Chemical Company, Germany. N,N-Dimethylacetamide (DMAc) was purchased from Merck, Germany and lithium chloride (LiCl) was supplied by Across, Belgium.

### Acid Hydrolysis of OPEFB (Untreated PEFB)

Four percent NaOH solution was used to treat OPEFB at a temperature of 70 °C for 3 h under stirring. This procedure was repeated three times. The bleaching treatment was conducted to remove residual lignin. The treatment was done in an acetate buffer (solution of 2.7 g NaOH and 7.5 mL acetic acid in 100 mL distilled water), aqueous sodium chlorite ($NaClO_2$) (1.7 % w/v), and was performed at 80 °C for 4 h. The treated filler was subsequently filtered, washed, and dried. The acid hydrolysis using 65% sulfuric acid ($H_2SO_4$) at a temperature of 45 °C was conducted under stirring conditions. The reaction of OPEFB suspension was stopped using cold distilled water. When the pH of the treated OPEFB reached 7, the OPEFB was dried at a temperature of 70 °C for 1 day.

### Chemical Treatment of OPEFB with MAA (Treated OPEFB)

The chemical used for treatment of OPEFB was methacrylic acid (MAA). Three percent MAA was dissolved in ethanol (v/v). The solution was stirred for a few minutes before OPEFB was added, then the mixture was stirred for 2 h. The solution was left overnight. Then, the treated OPEFB was dried at 70 °C for 24 h.

### Preparation of Untreated and Treated OPEFB Regenerated Cellulose Biocomposite Films

OPEFB with ratios of 1, 2, 3, and 4 wt.% and 3 wt.% MCC were first activated for 5 h in distilled water at room temperature. The swollen MCC and OPEFB were dehydrated in acetone and DMAc for 5 and 4 h, respectively. Then, the activated OPEFB and MCC were dissolved in DMAc for 20 min. LiCl at 8 wt.% was then added, and the solution was stirred for another 40 min, until the LiCl completely dissolved into the solution. The

regenerated cellulose solution was then poured onto a glass plate. The biocomposite films were washed with distilled water to remove the residual DMAc/LiCl solution. The transparent regenerated cellulose biocomposite films were dried at room temperature for 1 day. Table 1 shows the formulation for untreated and treated OPEFB regenerated cellulose biocomposite films.

**Table 1.** Formulation of Untreated and Treated OPEFB Regenerated Cellulose Biocomposite Films

| Materials | Untreated OPEFB Regenerated Cellulose Biocomposite Films | Treated OPEFB Regenerated Cellulose Biocomposite Films with MAA |
|---|---|---|
| Microcrystalline cellulose (MCC) (wt.%) | 3 | 3 |
| Regenerated cellulose (OPEFB) (wt.%) | 1, 2, 3, 4 | 1, 2, 3, 4 |
| Methacrylic acid (MAA) (%) | - | 3 |

## Tensile Properties

The tensile test was conducted using an Instron Universal Testing Machine, Model 5569, USA. The tensile test was according to ASTM D 882, with a cross-head speed of 10 mm/min. The tensile strength, elongation at break, and modulus of elasticity were recorded using the computer software.

## X-Ray Diffraction (XRD)

X-ray diffraction was conducted using an X-ray diffractometer model Bruker D8 Advance, USA, with Cu-Kd ($\lambda$ = 1.5418 Å) as the X-ray source. The crystallinity index (CrI) for both untreated and treated RC biocomposite films was calculated based on Eq. 1 (Ghaderi *et al.* 2014),

$$\text{Crystallinity Index (CrI)} = (I - I') / (I) \times 100\ \% \quad (1)$$

where $I$ is the height of the peak assigned to (200) planes, located in the range $2\theta$ = 20° to 23°, and $I'$ is the height of the peak assigned to (100) planes, measured at $2\theta$ = 12° to 16°, which is where the measurement occurred in the diffractogram.

## Morphology Study

The morphology study was carried out using a scanning electron microscope (SEM), model JEOL JSM-6460LA, Japan. The samples were coated using an Auto Fine Coater JFC -1600, Japan with a thin layer of palladium. The SEM was operated at a voltage of 10 kV.

## Thermogravimetric Analysis (TGA)

The thermal properties of RC biocomposite films were measured using TGA Pyris Diamond Perkin Elmer, Germany. The analysis conditions were as follows: a nitrogen atmosphere with a flow rate of 50 mL/min under the temperature range 25 to 700 °C and a heating rate of 10 °C/min.

### Fourier Transform Infrared Spectroscopy (FTIR)

The analysis of the functional groups of untreated and treated RC biocomposite films was carried out using a Perkin Elmer, Model L1280044 (Germany). The KBr method and attenuated total reflectance (ATR) method were used. The samples were scanned sixteen times in the wavenumber range of 4000 to 600 $cm^{-1}$ with a resolution of 4 $cm^{-1}$.

## RESULTS AND DISCUSSION

### Tensile Strength

Figure 1 illustrates the effect of OPEFB content on the tensile strength of untreated and treated RC biocomposite films with MAA. The tensile strength of untreated and treated RC biocomposite films increased with up to 2 wt.% OPEFB content and decreased with more than 3 wt.% OPEFB content. The tensile strength of 2 wt.% OPEFB untreated RC biocomposite films increased because the OPEFB particles were partially dissolved and dispersed in the solvent. As OPEFB content increased, the tensile strength decreased due to the aggregation of OPEFB particles. From Fig. 1, it can be seen that at similar contents of OPEFB, the tensile strength for treated RC biocomposite films with MAA was higher than for untreated RC biocomposite films. The highest tensile strength of treated RC biocomposite films was found at 2 wt.% OPEFB content. The increment of treated biocomposite films at 2 wt.% OPEFB content is 18.2% from the untreated biocomposite films. The MAA treatment reduced the surface polarity (intra and inter linkage) of OPEFB by reacting MAA with the hydroxyl group of cellulose from OPEFB. Furthermore, it improved the filler-matrix adhesion and the interaction of the biocomposite films.

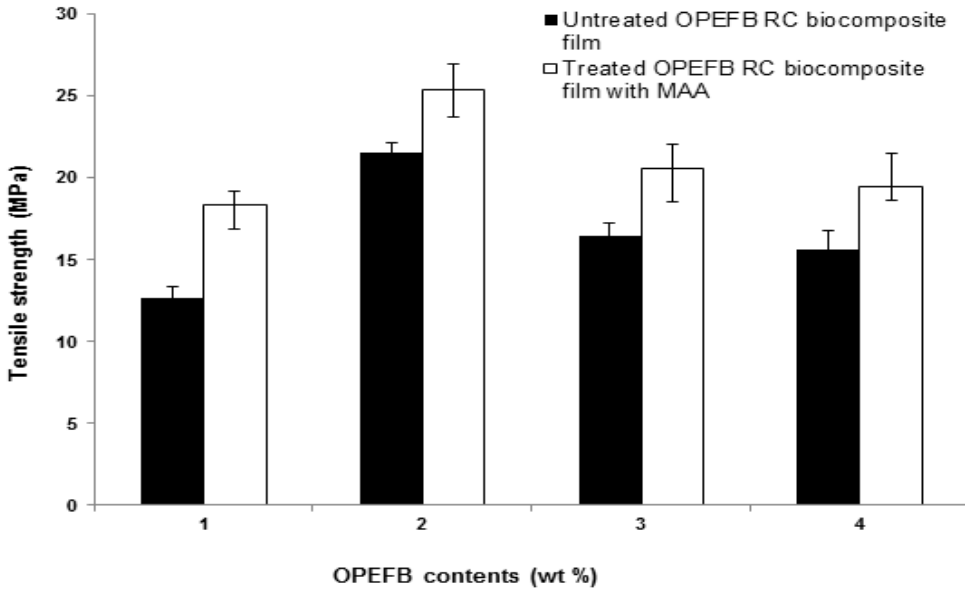


**Fig. 1.** The effect of OPEFB content on the tensile strength of untreated and treated RC biocomposite films with MAA

The effect of OPEFB content on the elongation at break of untreated and treated RC biocomposite films with MAA is shown in Fig. 2. The elongation at break for both untreated and treated biocomposite films decreased slightly when OPEFB content

increased from 1 to 2 wt.%. Furthermore, the elongation at break for both biocomposite films increased with more than 3 wt.% OPEFB content. The decreased elongation at break of untreated RC biocomposite films at 2 wt.% could be attributed to the presence of OPEFB, which strained the slippage movement of the RC chain, thus decreasing chain mobility. It was found that the treated RC biocomposite films exhibited lower elongation at break than the untreated biocomposite films. The lower elongation at break of treated RC biocomposite films at 2 wt.% OPEFB content was caused by the restriction of the chain mobility of RC particles and the strong interfacial bonding between the filler and matrix, resulting in higher brittleness of the biocomposite films.

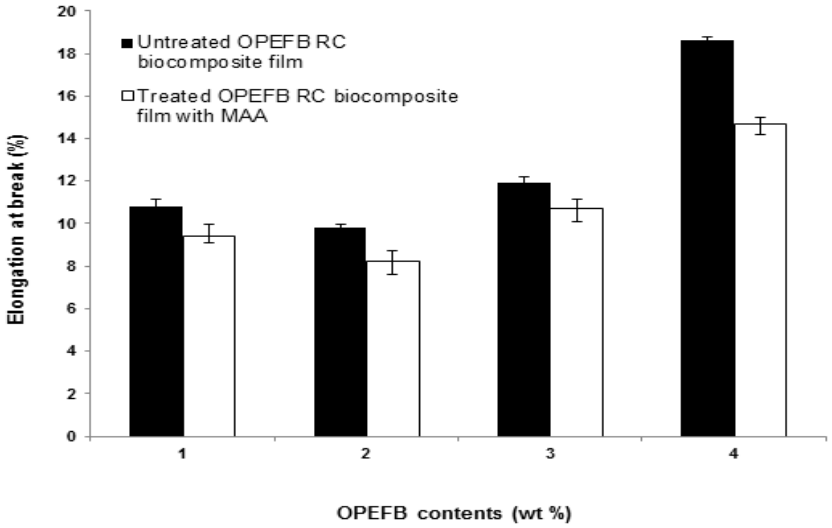


**Fig. 2.** The effect of OPEFB content on the elongation at break of untreated and treated RC biocomposite films with MAA

Figure 3 presents the effect of OPEFB content on the modulus of elasticity of untreated and treated RC biocomposite films with MAA.

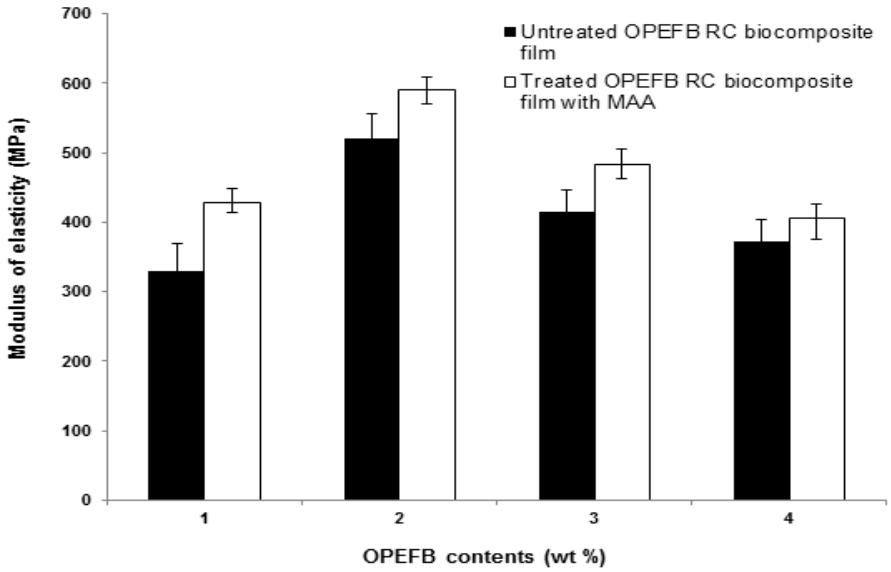


**Fig. 3.** The effect of OPEFB content on the modulus of elasticity of untreated and treated RC biocomposite films with MAA

The modulus of elasticity of both biocomposite films exhibited a similar trend of increasing at 1 and 2 wt.% OPEFB contents and decreasing at higher OPEFB contents. At similar OPEFB contents, the treated RC biocomposite films had a higher modulus of elasticity than untreated RC biocomposite films. The increment of modulus of elasticity at 2 wt.% OPEFB content was 29.2%. The presence of MAA improved the dispersion and adhesion of treated RC biocomposite films, thus enhancing the interfacial interaction and increasing the stiffness of treated RC biocomposite films. This is directed towards the treatment with MAA, which has intrinsic brittleness with OPEFB.

## X-Ray Diffraction (XRD)

The XRD curves of untreated and treated RC biocomposite films at different OPEFB contents are presented in Fig. 4. Table 2 shows the crystallinity index (CrI) for both untreated and treated OPEFB RC biocomposite films.

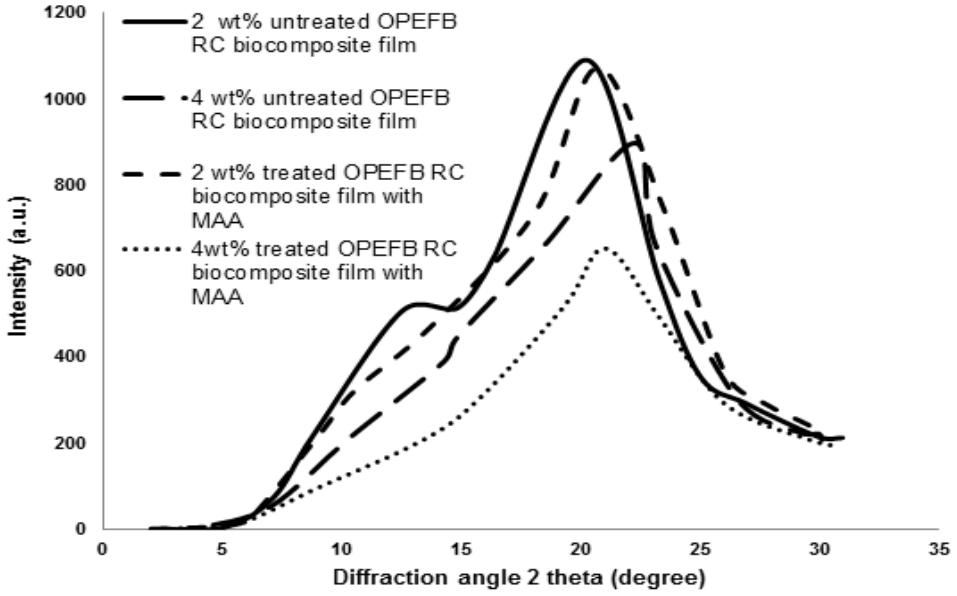


**Fig. 4.** XRD curves of untreated and treated RC biocomposite films at different OPEFB contents

**Table 2.** Crystallinity Index (CrI) of Untreated and Treated OPEFB RC Biocomposite Films with MAA

| Biocomposite Films | Untreated | | | Treated | | |
|---|---|---|---|---|---|---|
| | 2$\theta$(100) | 2$\theta$(200) | Crystallinity Index (CrI) (%) | 2$\theta$(100) | 2$\theta$(200) | Crystallinity Index (CrI) (%) |
| 1 wt.% OPEFB RC biocomposite films | 16.18 | 20.40 | 43.96 | 16.58 | 21.12 | 49.37 |
| 2 wt.% OPEFB RC biocomposite films | 14.84 | 21.94 | 52.84 | 14.95 | 22.45 | 56.16 |
| 3 wt.% OPEFB RC biocomposite films | 15.02 | 20.93 | 51.93 | 14.89 | 21.71 | 54.46 |
| 4 wt.% OPEFB RC biocomposite films | 14.82 | 20.25 | 50.28 | 12.13 | 21.03 | 52.91 |

The peak for 2 wt.% OPEFB untreated RC biocomposite films was wider compared with 4 wt.% of OPEFB untreated RC biocomposite films, as shown in Fig. 4. This indicates the formation of cellulose II from cellulose I during dissolution in the solvents (Pang *et al*. 2013). As can be seen in Table 2, the crystallinity index (CrI) of treated RC biocomposite film treatment with MAA was higher than the untreated biocomposite films. The increase in OPEFB content led to an increase in the cellulose crystallinity of treated biocomposite films. At 2 wt.% OPEFB, treated RC biocomposite films exhibited a higher CrI value than other OPEFB RC biocomposite films.

## Morphology Study

Figures 5 and 6 show SEM tensile surface fracture for untreated and treated RC biocomposite films at 2 wt.% OPEFB content. As can be seen in Fig. 5, the surface fracture of untreated RC biocomposite films showed some voids and agglomerations.

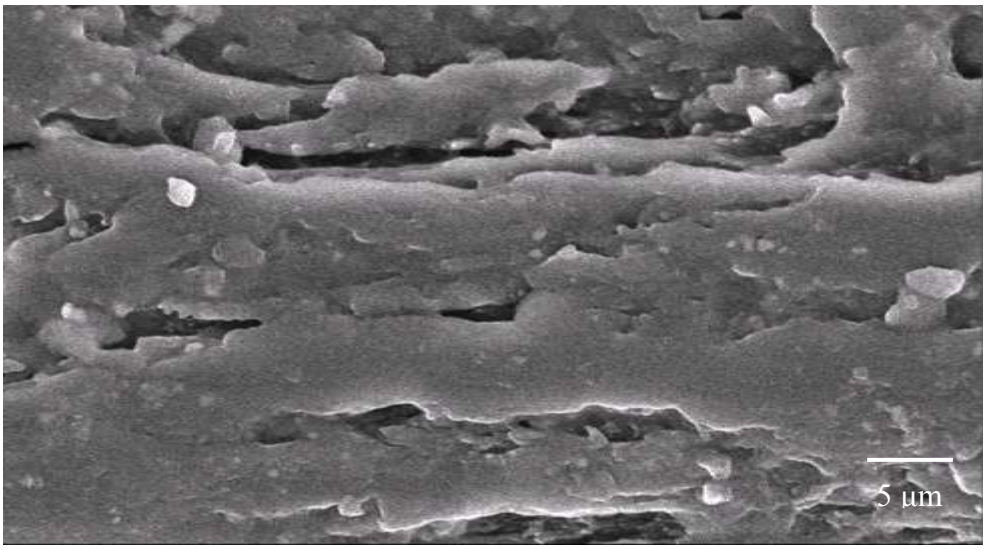


**Fig. 5.** SEM micrograph of the tensile surface fracture of untreated RC biocomposite films at 2 wt.% of OPEFB

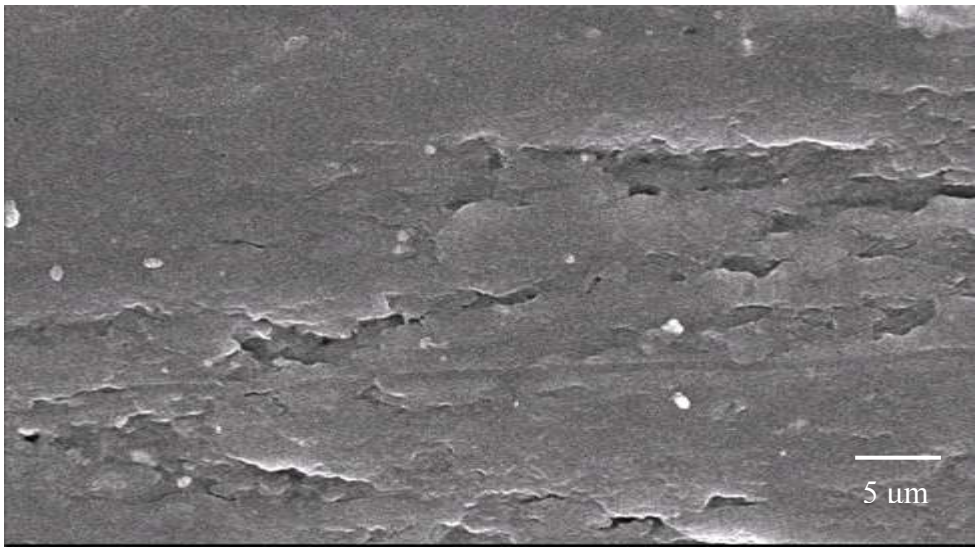


**Fig. 6.** SEM micrograph of tensile surface fracture of treated RC biocomposite films with MAA at 2 wt.% of OPEFB

Figure 6 shows that the surface fracture of treated RC biocomposite films showed more homogeneity, with less voids and agglomerations occurring. The treated RC biocomposite films with MAA showed better dispersion and adhesion of the OPEFB filler and OPEFB matrix. This was demonstrated by the tensile strength values of treated RC biocomposite films, which were higher than those of untreated RC biocomposite films, as discussed previously.

## Thermogravimetric Analysis (TGA)

Figure 7 presents the thermogravimetric analysis (TGA) curves of untreated and treated RC biocomposite films with MAA at 2 wt.% OPEFB content. The TGA data of untreated and treated RC biocomposite films are shown in Table 3. As shown in the table, the temperature maximum degradation ($T_{dmax}$) of untreated RC biocomposite films decreased with increasing OPEFB content.

The weight loss of untreated RC biocomposite films with temperature degradation at 300 °C ($T_{300}$) decreased as OPEFB content increased. The weight loss of 4 wt.% OPEFB content of untreated RC biocomposite films was higher than that of 2 wt.% with temperature degradation at 600 °C ($T_{600}$).

It was found that the treated biocomposite films showed higher $T_{dmax}$ than the untreated RC biocomposite films. The weight loss with temperature degradation at 300 °C ($T_{300}$) and 600 °C ($T_{600}$) of treated RC biocomposite films was lower compared with that of untreated RC biocomposite films. This is because the MAA treatment of OPEFB increased the thermal stability of the RC biocomposite films. This shows that the treated RC biocomposite films with MAA were resistant to thermal degradation at higher temperatures.

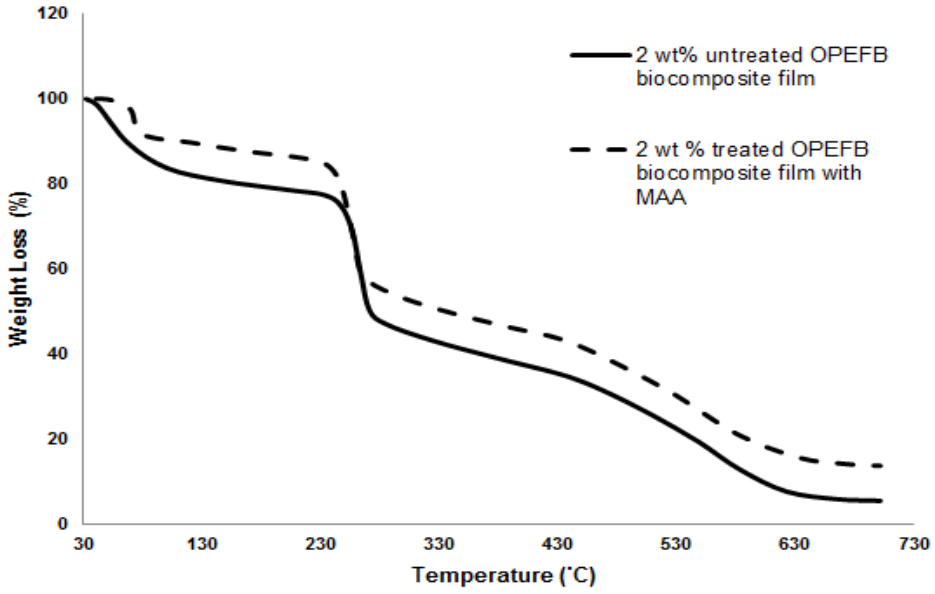


**Fig. 7.** Thermogravimetric analysis (TGA) curves of untreated and treated RC biocomposite films with MAA at 2 wt.% OPEFB content

**Table 3.** TGA Data of Untreated and Treated RC Biocomposite Films with MAA at 2 and 4 wt.% of OPEFB Content

| **RC Biocomposite Films** (wt.%) | $T_{dmax}$ (°C) | **Weight loss** (%) | |
|---|---|---|---|
| | | 300 °C | 600 °C |
| 2 wt.% OPEFB RC biocomposite films (untreated) | 261.8 | 54.49 | 89.78 |
| 4 wt.% OPEFB RC biocomposite films (untreated) | 255.03 | 50.75 | 91.08 |
| 2 wt.% OPEFB RC biocomposite films (treated with MAA) | 262.65 | 46.71 | 86.42 |
| 4 wt.% OPEFB RC biocomposite films (treated with MAA) | 269.6 | 50.25 | 89.49 |

## Fourier Transform Infrared Spectroscopy Analysis (FTIR)

The FTIR spectra for the untreated and treated OPEFB RC biocomposite films with MAA are presented in Fig. 8. The peaks at 3377 $cm^{-1}$ for both untreated and treated RC biocomposite films showed the presence of the –OH group. The CH-stretching was represented by the peak at 2920 $cm^{-1}$ for untreated RC biocomposite films and 2906 $cm^{-1}$ for treated RC biocomposite films. The carbonyl group from cellulose was shifted from 1643 $cm^{-1}$ of untreated RC biocomposite films to 1652 $cm^{-1}$ of treated RC biocomposite films. The peak at 1376 $cm^{-1}$ and 1337 $cm^{-1}$ indicates the CH-stretching of cellulose and hemicelluloses. The cleavage of the band 1157 $cm^{-1}$ in untreated OPEFB RC biocomposite films refers to the C-O bond. The spectrum for untreated RC biocomposite films at 899 $cm^{-1}$ and treated RC biocomposite films at 890 $cm^{-1}$ represent the glycosidic $C_1$-H deformation with a ring vibration contribution indicative of β-glycosidic linkages between the units of sugar. The peak at 1023 $cm^{-1}$ was shifted to 1041 $cm^{-1}$ for the C-O group, indicating bonding between the OPEFB cellulose and the MAA treatment. The schematic reaction between OPEFB cellulose with MAA treatment is illustrated in Fig. 9.

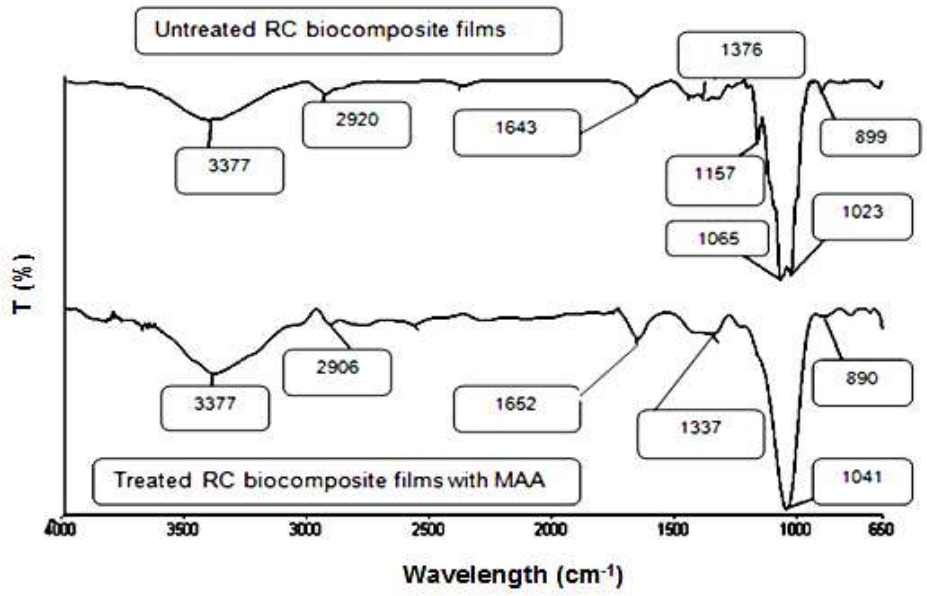


**Fig. 8.** FTIR spectra of untreated and treated OPEFB RC biocomposite films with MAA

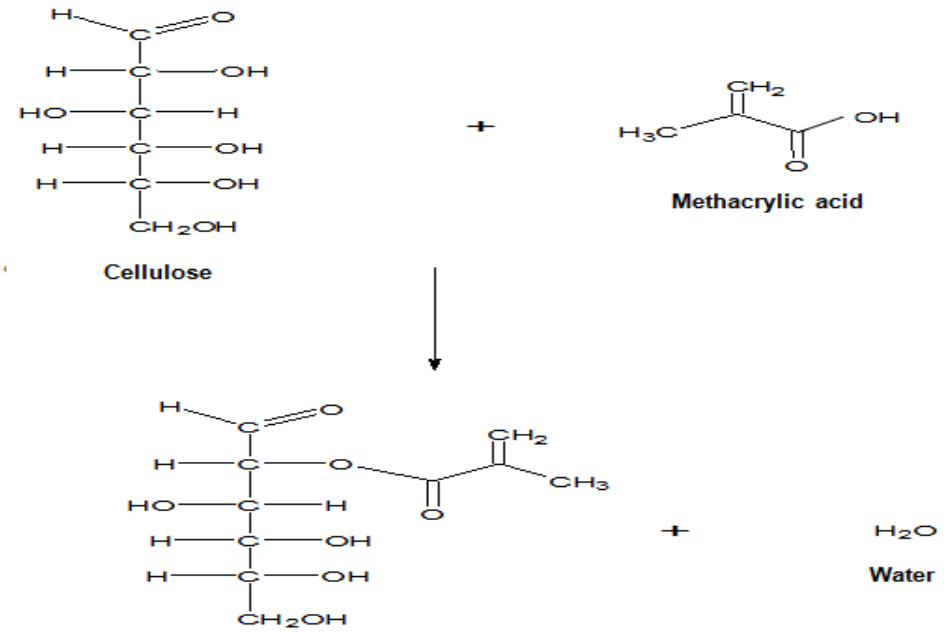


**Fig. 9.** Schematic of reaction between OPEFB cellulose with MAA treatment

## CONCLUSIONS

1. At 2 wt.% OPEFB content, untreated RC biocomposite films had the highest crystallinity index (CrI) value compared with other untreated RC biocomposite films. In addition, the tensile strength and modulus of elasticity for 2 wt.% OPEFB content of untreated RC biocomposite films showed higher results, while the elongation at break was found to be lower. The thermogravimetric analysis (TGA) results showed that both $T_{dmax}$ and weight loss at 300 °C ($T_{300}$) decreased with increasing OPEFB content, whereas the weight loss at 600 °C ($T_{600}$) tended to increase.
2. The OPEFB RC biocomposite films treated with MAA showed higher crystallinity index (CrI), tensile strength, and modulus of elasticity compared with the untreated RC biocomposite films, but lower elongation at break. At 2 wt.% OPEFB content, treated RC biocomposite films indicated the highest crystallinity index compared with other OPEFB contents. The tensile strength and modulus of elasticity was also higher for 2 wt.% OPEFB content treated RC biocomposite films.
3. The SEM micrograph tensile surface fracture of treated OPEFB RC biocomposite films at 2 wt.% OPEFB content exhibited better dispersion of the OPEFB into the matrix of the RC biocomposite. The chemical treatment with MAA increased the $T_{dmax}$ of treated RC biocomposite films. RC biocomposite films treated with MAA had higher thermal stability.

## REFERENCES CITED

Ariffin, H., Hassan, M. A., Umi Kalsom, M. S., Abdullah, N., and Shirai, Y. (2008). "Effect of physical, chemical and thermal pretreatments on the enzymatic hydrolysis of oil palm empty fruit bunch (OPEFB)," *J. Trop. Agric. Food Sci.* 36(2), 1-10.

ASTM D882-12 (2012). "Standard test method for tensile properties of thin plastic sheeting," ASTM International, West Conshohocken, PA.

Biganska, O., and Navard, P. (2002). "Crystallization of cellulose/N-methylmorpholine-N-oxide solution," *Polymer* 43(23), 6139-6145. DOI: 10.1016/S0032-3861(02)00552-9

Chang, S. H. (2014). "An overview of empty fruit bunch from oil palm as feedstock for bio-oil production," *Biomass Bioenerg.* 62, 174-181. DOI: 10.1016/j.biombioe.2014.01.002

Dulchemin, B. J. C., Mathew, A. P., and Osman, K. (2009). "All-cellulose composites by partial dissolution in the ionic liquid 1-butyl-3-methylimidazolium chloride," *Compos. Part A* 40(12), 2031-2037. DOI: 10.1016/j.compositesa.2009.09.013

Geng, A. (2013). "Conversion of oil palm empty fruit bunch to biofuels, liquid, gaseous and solid biofuels," in: *Conversion Techniques*, Z. Fang (ed.), InTech, Croatia, pp. 479-490. DOI: 10.5772/53043

Ghaderi, M., Mousavi, M., Yousefi, H., and Labbafi, M. (2014). "All-cellulose nanocomposite film made from bagasse cellulose nanofibers for food packaging application," *Carbohydr. Polym.* 104, 59-65. DOI: 10.1016/j.carbpol.2014.01.013

Huber, T., Mussig, J., Curnow, O., Pang, S., Bickerton, S., and Staiger, M. P. (2012). "A critical review of all-cellulose composites," *J. Mater. Sci.* 47(3), 1171-1186. DOI: 10.1007/s10853-011-5774-3

Kalia, S., Dufresne, A., Cherian, B. M., Kaith, B. S., Avérous, L., and Njuguna, J. (2011). "Cellulose-based bio and nanocomposites: A review," *Int. J. Polym. Sci.* 837875. DOI: 10.1155/2011/837875

Kmelty, A., Baramy, T., and Karger-Kocsis, J. (2010). "Self-reinforced polymeric materials: A review," *Prog. Polym. Sci.* 35(10), 1288-1310. DOI: 10.1016/j.progpolymsci.2010.07.002

Li, X., Tabil, L. G., and Saryanarayan, P. (2007). "Chemical treatments of natural fiber for use in natural fiber. Reinforced composites: A review," *J. Polym. Environ.* 15(1), 25-33. DOI: 10.1007/s10924-006-0042-3

Liu, Z., Sun, X., Hao, M., Huang, C., Xue, Z., and Mu, T. (2015). "Preparation and characterization of regenerated cellulose from ionic liquid using different methods," *Carbohydr. Polym.* 117, 99–105. DOI: 10.1016/j.carbpol.2014.09.053

Nishino, T., Natsuda, I., and Hirou, K. (2004). "All-cellulose composite," *Macromolecules* 37(20), 7683-7687. DOI: 10.1021/ma049300h

Nishiyama, Y., Langan, P., and Chanzy, H. (2002). "Crystal structure and hydrogen-bonding system in cellulose Iβ from synchrotron X-ray and neutron fiber diffraction," *J. Am. Chem. Soc.* 124(31), 9074-9082. DOI: 10.1021/ja0257319

Pang, J., Liu, X., Zhang, X., Wu, Y., and Sun, R. (2013). "Fabrication of cellulose film with enhanced mechanical properties in ionic liquid 1-allyl-3-methylimidaxolium chloride (AmimCl)," *Materials* 6(4), 1270-1284. DOI: 10.3390/ma6041270

Röder, T., Moosbauer, J., Kliba, G., Schlader, S., Zuckerstätter, G., and Sixta, H. (2009). "Comparative characterisation of man-made regenerated cellulose fibres," *Lenzinger Berichte* 87, 98-105.

Sahari, J., and Sapuan, S. M. (2011). "Natural fibre reinforced biodegradable polymer composites," *Rev. Adv. Mater. Sci.* 30(2), 166-174.

Soheilmoghaddam, M., Wahit, M. U., Yusuf, A. A., al-Saleh, M. A. and Whye, W. T. (2014a). "Characterization of bioregenerated cellulose/sepiolite nanocomposite films prepare *via* ionic liquid," *Polym. Test.* 33, 121-130. DOI: 10.1016/j.polymertesting.2013.11.011

Soheilmoghaddam, M., Wahit, M. U., Whye, W. T., Akos, N. I., Pour, R. H. and Yussuf, A. A. (2014b). "Bionanocomposites of regenerated cellulose/zeolite prepared using environmentally benign ionic liquid solvent," *Carbohydr. Polym.* 106, 326-334. DOI: 10.1016/j.carbpol.2014.02.085

Sulaiman, F., Abdullah, N., Gerhauser, H., and Shariff, A. (2011). "An outlook of Malaysian energy, oil palm industry and its utilization of wastes as useful resources," *Biomass Bioenerg.* 35(9), 3775-3786. DOI: 10.1016/j.biombioe.2011.06.018

Ward, I., and Hine, P. J. (2004). "The science and technology of hot compaction," *Polymer* 45(5), 1413-1427. DOI: 10.1016/j.polymer.2003.11.050

Zhang, X., Feng, J., Liu, X., and Zhu, J. (2012). "Preparation and characterization of regenerated cellulose/poly (vinylidene fluoride) (PVDF) blend films," *Carbohydr. Polym.* 89, 67-71. DOI: 10.1016/j.carbpol.2012.02.047

Zhao, H., Kwak, J. H., Wang, Y., Franz, J. A., White, J. M., and Holladay, J. E. (2007). "Interactions between cellulose and N-methylmorpholine-N-oxide," *Carbohydr. Polym.* 67(1), 97-103. DOI: 10.1016/j.carbpol.2006.04.019

Zhao, J., He, X., Wang, Y., Zhang, W., Zhang, X., Zhang, X., Deng, Y., and Lu, C. (2014). "Reinforcement of all-cellulose nanocomposite films using native cellulose nanofibrils," *Carbohydr. Polym.* 104, 143-150. DOI: 10.1016/j.carbpol.2014.01.007

Article submitted: August 19, 2015; Peer review completed: November 1, 2015; Revised version received: Nobember 8, 2015; Accepted: November 9, 2015; Published: November 30, 2015.
DOI: 10.15376/biores.11.1.873-885